Ethanol Oxidation: Kinetics of the α-Hydroxyethyl Radical + O_2 Reaction

Gabriel da Silva,[†] Joseph W. Bozzelli,*[,‡] Long Liang,[§] and John T. Farrell[§]

Department of Chemical and Biomolecular Engineering, The University of Melbourne, Victoria 3010, Australia, Department of Chemistry and Environmental Science, New Jersey Institute of Technology, Newark, New Jersey 07102, Corporate Strategic Research Laboratories, ExxonMobil Research and Engineering Company, Annandale, New Jersey 08801

Received: April 7, 2009; Revised Manuscript Received: May 28, 2009

Bioethanol is currently a significant gasoline additive and the major blend component of flex-fuel formulations. Ethanol is a high-octane fuel component, and vehicles designed to take advantage of higher octane fuel blends could operate at higher compression ratios than traditional gasoline engines, leading to improved performance and tank-to-wheel efficiency. There are significant uncertainties, however, regarding the mechanism for ethanol autoignition, especially at lower temperatures such as in the negative temperature coefficient (NTC) regime. We have studied an important chemical process in the autoignition and oxidation of ethanol, reaction of the α-hydroxyethyl radical with $O_2(^3P)$, using first principles computational chemistry, variational transition state theory, and Rice−Ramsperger−Kassel−Marcus (RRKM)/master equation simulations. The α-hydroxyethyl + O_2 association reaction is found to produce an activated α-hydroxy−ethylperoxy adduct with ca. 37 kcal mol^{-1} of excess vibrational energy. This activated adduct predominantly proceeds to acetaldehyde + HO_2, with smaller quantities of the enol vinyl alcohol (ethenol), particularly at higher temperatures. The reaction to acetaldehyde + HO_2 proceeds with such a low barrier that collision stabilization of $C_2O_3H_5$ isomers is unimportant, even for high-pressure/low-temperature conditions. The short lifetimes of these radicals precludes the chain-branching addition of a second O_2 molecule, responsible for NTC behavior in alkane autoignition. This result helps to explain why ignition delays for ethanol are longer than those for ethane, despite ethanol having a weaker C−C bond energy. Given its relative instability, it is also unlikely that the α-hydroxy−ethylperoxy radical acts as a major acetaldehyde sink in the atmosphere, as has been suggested.

Introduction

Worldwide use of bioethanol as a blend component for gasoline is increasing. In the U.S. this is due in part to legislation passed in 2007 that mandates the use of 36 billion gallons of biofuels per year by 2022. Ethanol blends at levels up to 10% (E10) can be used in all current gasoline light-duty vehicles sold in the U.S. and can be dispensed from existing U.S. service station pumps and tanks. Flex-fuel vehicles, capable of operating on fuels containing up to 85% ethanol (E85), are becoming more widespread. Considerable efforts are being directed toward modeling the combustion of ethanol and ethanol blends, in order to help improve engine performance and efficiency.

Ethanol demonstrates significant resistance to engine knock, which is unwanted autoignition of the fuel−air charge ahead of the propagating flame front. The research octane number (RON) of ethanol, a measure of antiknock behavior, is 116 (compared to around 95 for a typical gasoline formulation). The high octane rating of ethanol is beneficial in that it could allow future flex-fuel vehicles to operate with more advanced spark timing or at higher effective compression ratios when operating on E85. Even though ethanol contains less chemical (potential) energy than gasoline, it may be possible to extract a similar or greater quantity of mechanical energy from flex-fuel vehicles, once optimized to take advantage of ethanol's high octane rating, as well as the greater cooling effect due to the high latent heat of vaporization. To realize such efficiency gains, detailed chemical kinetic models are required for the autoignition and oxidation of ethanol, as well as a thorough fundamental understanding of ignition phenomena. Bioethanol is also a promising fuel component for use in next-generation HCCI (homogeneous charge compression ignition) engines, which achieve efficiencies comparable to diesel (compression ignition) engines, but with the improved emissions of a gasoline (spark ignition) engine. HCCI engines operate through autoignition of the compressed fuel−air charge, and modeling of the chemical phenomena involved in autoignition is proving integral to the implementation of these advanced engines.

The high octane rating and relatively long ignition delays associated with ethanol have not been fully explained or modeled in the scientific literature. In 1971, Cooke et al.[1] studied ethanol and methanol autoignition. Ignition of methanol (CH_3OH) was explained by initial fission of the CH_3-OH bond, and to a lesser extent the stronger $H-CH_2OH$ bonds (respective bond dissociation energies, BDEs, are 92.0 and 96.1 kcal mol^{-1}).[2−7] Ethanol (CH_3CH_2OH) ignition was attributed to dissociation of the relatively weak CH_3-CH_2OH bond[1] (BDE = 87.2 kcal mol^{-1}).[4,5,7] This hypothesis was supported by the longer ignition delays measured for methanol versus ethanol. However, ignition delays for ethanol are longer than those for ethane (CH_3CH_3) and appear to diverge with decreasing temperature,[1] despite the ethanol CH_3-CH_2OH bond being significantly weaker than the ethane CH_3-CH_3 bond (BDE = 90.1 kcal mol^{-1}).[5,8] This result was not explained at the time, nor has it been explained since.

* To whom correspondence should be addressed. E-mail: bozzelli@njit.edu.
[†] The University of Melbourne.
[‡] New Jersey Institute of Technology.
[§] ExxonMobil Research and Engineering Company.

10.1021/jp903210a CCC: $40.75
Published on Web 07/13/2009

Since these early studies, considerable progress has been made toward modeling the ignition and combustion behavior of ethanol, especially at high temperatures. Dunphy et al.[9] presented a reaction mechanism for ethanol oxidation above 1000 K, which they used to model ignition delays in ethanol combustion.[10] The model was relatively successful at higher temperatures but showed significant discrepancies at the lower temperature range, being too slow by a factor of around 1−3 at 1250 K. Rate constant optimization managed to significantly improve the modeling of ignition delay times, although this is not necessarily due to an improved description of the fundamental reaction kinetics. A sensitivity analysis identified CH_3-CH_2OH bond dissociation as being important in ethanol ignition, as hypothesized by Cooke and co-workers,[1] although this reaction was much less important at the lower end of the temperature range (1250 K). In 1999 Marinov[11] presented a comprehensive model for ethanol oxidation, featuring 369 reactions (almost four times the number used by the Simmie group). Again, ignition delays were well-reproduced by the model. The most sensitive reaction in the ethanol submechanism was for dissociation of ethanol to $CH_3 + CH_2OH$, followed by the reactions of these radicals with HO_2 and O_2, respectively. The model was also sensitive to the dissociation of ethanol to $CH_3CH_2 + OH$. More recent work on the thermal decomposition of ethanol has identified that initial C−C bond scission reactions, as well as subsequent abstraction reactions between the produced radicals and ethanol, are important.[12,13] Research is still required to understand and accurately model the oxidation and autoignition of ethanol, especially for temperatures in the range of 600−1000 K, relevant to two-stage ignition and negative temperature coefficient (NTC) behavior.

An important initial process in the oxidation of ethanol is well-known to be abstraction of ethanol hydrogen atoms by species in the active radical pool. Hydrogen abstraction in ethanol can occur from the OH group (CH_3CH_2O-H) or from an α ($CH_3CH(-H)OH$) or β ($CH_2(-H)CH_2OH$) carbon site. These reactions are reasonably well characterized, both thermodynamically and kinetically. The weakest hydrogen in ethanol is on the α carbon, with a C−H BDE of 95.2 kcal mol^{-1}, versus 102.5 kcal mol^{-1} for the β C−H bond and 104.1 kcal mol^{-1} for the O−H bond,[14] and branching ratio analysis reveals that the α-hydroxyethyl radical ($CH_3C^{\bullet}HOH$) is the dominant abstraction product from ethanol, especially at lower temperatures.[11] In this contribution we study the chemically activated association of this important radical with O_2, using first principles computational chemistry and statistical rate theory. The results of this study will help to explain and model the anomalous autoignition behavior of ethanol. The α-hydroxyethyl + O_2 reaction is currently included in the Marinov kinetic model for ethanol oxidation[11] [where k/(cm^3 mol^{-1} s^{-1}) = $4.82 \times 10^{14}\exp(-2525/(T/\mathrm{K}))$], but the kinetics and products are estimated from the analogous hydroxymethyl + O_2 reaction system, where several potentially important pathways are unavailable. A theoretical study of this reaction has been recently presented,[15] where the new, calculated rate constants are in significant disagreement with those currently used to model ethanol oxidation at temperatures above 1000 K.

In addition to their role in alcohol oxidation mechanisms, the reactions of hydroxyalkyl radicals with O_2 are also of importance to atmospheric chemistry. The hydroxymethyl radical is often used as a hydroxyalkyl radical analogue and is therefore relatively well studied. Experimentally this reaction is found to produce formaldehyde (CH_2O) + HO_2,[16] with rate constants on the order of 4×10^{12} cm^3 mol^{-1} s^{-1} at room temperature, and a small negative temperature dependence. Theoretical studies of this reaction support an O_2 addition,−H_2O elimination mechanism.[16,17] The α-hydroxyalkylperoxy radicals are important intermediates in the atmospheric oxidation of aldehydes and ketones,[18] where they are thought to act as sinks for these ketonyl compounds. In the context of atmospheric chemistry, modeling of the hydroxyethyl + O_2 reaction system is important in extrapolating from the reactions of hydroxymethyl to hydroxyalkyl radicals, where differences in the total reaction rate are expected, while additional and potentially important reaction pathways will become available. The present work further relates to atmospheric chemistry because of the involvement of the reaction products acetaldehyde and vinyl alcohol in atmospheric processes. It has been recently suggested that increased use of E85 could increase ozone-related mortalities and medical incidents, principally due to drastically increased acetaldehyde emissions.[19] Vinyl alcohol, an intermediate which has been identified in ethanol flames,[20] and is revealed here to be a product of the α-hydroxyethyl + O_2 reaction (vide infra), has been suggested as a significant tropospheric source of carboxylic acids.[21] Low molecular weight carboxylic acids are major contributors to acid rain[22] but are currently underpredicted by atmospheric chemistry models.

Methods

Quantum Chemical Calculations. Ab initio and density functional theory (DFT) calculations were performed with the Gaussian 03 program suite.[23] All identified minima and transition states on the $C_2H_5O_3$ potential energy surface were calculated using the G3B3 composite theoretical method.[24] The G3B3 method uses B3LYP/6-31G(d) DFT geometries and frequencies, with higher level single-point ab initio energy corrections. All reported transition-state structures possessed a single imaginary frequency, where the mode of vibration of the imaginary frequency connected the stated reactants and products. The barrierless α-hydroxyethyl + O_2 and acetaldehyde + HO_2 association reactions were treated using variational transition state theory, as described below. Calculated enthalpies (hartrees), molecular geometries (in Cartesian coordinates), and vibrational frequencies are provided as Supporting Information for all stationary points.

Thermochemical Properties. Enthalpies of formation ($\Delta_f H°_{298}$) are reported for all minima and transition states. $\Delta_f H°_{298}$ values are determined at the G3B3 level from atomization work reactions, using 298 K literature enthalpies of formation of 171.435, 52.103, and 59.567 kcal mol^{-1} for the elements C, H, and O, respectively.[25] Thermochemical properties as a function of temperature (including $\Delta_f H°$, $S°$, and C_p) are evaluated from a molecule's 298 K enthalpy of formation, vibrational frequencies, and moments of inertia, according to statistical mechanical principles in the program ChemRate 1.5.2.[26] Vibrational frequencies corresponding to internal rotation were omitted from this analysis and were instead modeled as hindered internal rotors. Internal rotor potentials were calculated in all minima from relaxed scans at the B3LYP/6-31G(d) level of theory, to determine the barrier to rotation, number of rotational minima, and rotor symmetry. For transition states, internal rotors were modeled on the basis of reactant or product rotor potentials. In this study, C−OO$^{\bullet}$ internal rotation in all radicals and transition states is considered to be restricted by intramolecular interactions, and this degree of freedom is treated as a vibrational frequency.

Elementary Rate Parameters. For all elementary reactions, high-pressure-limit rate constants as a function of temperature

(k^{∞}) are calculated in ChemRate, according to canonical transition state theory. Corrections for symmetry, degeneracy, and optical isomers are incorporated where appropriate. Rate constants between 800 and 2000 K were fit to an empirical three-parameter form of the Arrhenius equation (eq 1) to obtain the high-pressure-limit elementary rate parameters A', n, and E_a. For reactions that predominantly involve an intramolecular hydrogen shift, rate constants are corrected for quantum mechanical tunneling according to Eckart theory.[27] All preexponential terms ($A'T^n$) quoted in this study are in units of s^{-1} (first order) or $cm^3\ mol^{-1}\ s^{-1}$ (second order), with all temperatures in K.

$$k = A'T^n \exp\left(\frac{-E_a}{RT}\right) \quad (1)$$

Variational Analysis. The α-hydroxyethyl + O_2 association reaction proceeds without any appreciable barrier in the forward direction, and the kinetics of this reaction therefore require treatment according to variational transition state theory (VTST). Additionally, the elimination reaction α-hydroxy−ethylperoxy → acetaldehyde + HO_2 is found to proceed via a hydrogen bonded acetaldehyde−HO_2 complex (similar to formaldehyde−HO_2), which also dissociates without a barrier. We have performed canonical variational transition state theory calculations for $k(T)$, with vibrator transition state structures used to obtain partition functions using the RRHO approximation, along with the inclusion of two internal rotational modes. The lack of conservation of angular momentum in our calculations is expected to lead to some overestimation of the rate constants.

The VTST procedure employed in this study is similar to that of da Silva and Bozzelli,[28] except here we utilize a UB3LYP/6-31G(d) potential energy scan of the dissociating C−OO bond in the α-hydroxy−ethylperoxy radical and the =O−O(H)O• bond in the acetaldehyde−HO_2 complex (in 0.1 Å steps). The B3LYP reaction energies between the points along the minimum energy potential (MEP) and the reactant were multiplied by a scaling factor of 1.03, which is the ratio of the G3B3 reaction enthalpy (37.4 kcal mol^{-1}) to the B3LYP 0 K reaction energy (36.4 kcal mol^{-1}). Heats of formation for structures along the MEP were obtained by adding the scaled reaction enthalpies to the α-hydroxy−ethylperoxy heat of formation. This procedure effectively uses the G3B3 calculations to provide the enthalpy of reaction and the results of the UB3LYP/6-31G(d) scan to approximate the shape of the MEP. Frequency calculations were performed for transition-state structures along the minimum energy pathways, yielding thermochemical properties as a function of temperature as described above.

Rate parameters were evaluated for the forward (association) and reverse (dissociation) reactions at each transition-state structure and minimized at each temperature in order to locate the variational transition state. In accordance with the principle of microscopic reversibility, the transition-state location as a function of temperature is seen to be the same for both the forward and reverse reaction processes. For the α-hydroxyethyl + O_2 reaction, the C−CH_3 and C−OH internal rotors in the transition-state structures were treated as hindered rotors, using rotor potentials calculated for the parent α-hydroxy−ethylperoxy radical. For the very loose transition-state structures, with C−OO bonds 3.39 Å or greater (where the vibrational frequency was less than 60 cm^{-1}), the C−OO internal rotor was modeled as a free rotor. For the acetaldehyde + HO_2 reaction, rotation about the C−CH_3 bond was modeled as a hindered internal rotation (modeled on the CH_3−CH=O rotor potential), while the acetaldehyde−HO_2 rotor was treated as a free internal rotation.

SCHEME 1: Proposed Mechanism for the α-Hydroxyethyl + O_2 Reaction

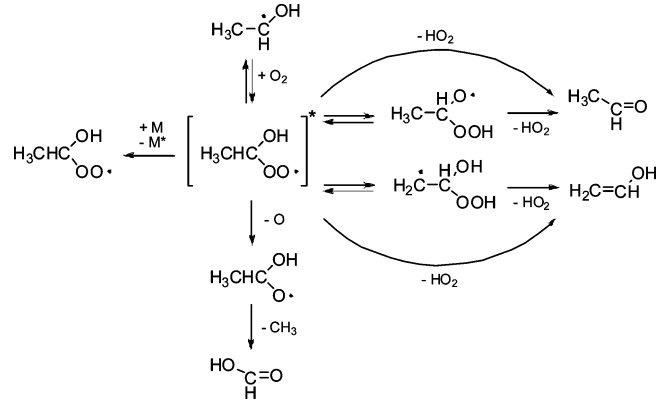

Kinetic Modeling. Branching ratios in the multichannel, multiwell α-hydroxyethyl radical + O_2 process are calculated using Rice−Ramsperger−Kassel−Marcus (RRKM) theory for $k(E)$, with master equation analysis for pressure falloff. Calculations are performed for $P = 0.001-100$ atm and $T = 300-2000$ K. A ΔE°_{down} value of 500 cm^{-1} was used in the master equation analysis, with N_2 as the third body. Rate constants, $k(E)$, were evaluated at 0.1 kcal mol^{-1} increments, up to 196 kcal mol^{-1} above the lowest energy isomer (around 160 kcal mol^{-1} above the highest barrier). Lennard-Jones parameters were estimated as $\sigma = 4.3$ Å and $\varepsilon/k_b = 489$ K. The results of this study are expected to be relatively insensitive to the parameters used in the RRKM/ME calculations, as the forward reaction to the major product set proceeds at around the α-hydroxyethyl + O_2 association rate for relevant combustion temperatures and pressures (vide infra).

Results and Discussion

Reaction Mechanism and Energy Diagram. The α-hydroxyethyl radical + O_2 reaction proceeds according to the mechanism depicted in Scheme 1. In this mechanism the α-hydroxyethyl radical reacts with O_2 to form the α-hydroxy−ethylperoxy radical ($CH_3CH_2(OO^{\bullet})OH^*$). This is a chemically activated adduct, which possesses 37.4 kcal mol^{-1} energy above the ground-state radical. This energy can go into further unimolecular reactions (including intramolecular hydrogen shift, elimination, and dissociation reactions), reverse reaction back to the α-hydroxyethyl radical + O_2, or can be lost via collisions with the bath gas (M), forming the stabilized α-hydroxy−ethylperoxy radical. From Scheme 1 we identify three sets of dissociation products in the α-hydroxyethyl + O_2 reaction: (i) acetaldehyde (CH_3CHO) + HO_2, (ii) vinyl alcohol (CH_2CHOH) + HO_2, and (iii) CH_3 + CH(OH)=O + O, in addition to the $C_2O_3H_5$ radical isomers α-hydroxy−ethylperoxy, α-hydroperoxy−ethoxy, and 2-hydroxy-2-hydroperoxy−1-ethyl. The reactions leading to each of these three product sets are discussed below. An energy diagram representing this reaction mechanism is provided as Figure 1.

(i) CH_3CHO + HO_2. In one pathway depicted in Scheme 1 (referred to as pathway I to CH_3CHO + HO_2), the α-hydroxy−ethylperoxy radical undergoes a concerted elimination reaction, providing acetaldehyde + HO_2 with a barrier of only 11.4 kcal mol^{-1} (26 kcal mol^{-1} below the entrance channel). This reaction pathway is analogous to the dominant addition−elimination pathway in the hydroxymethyl + O_2 reaction, which produces

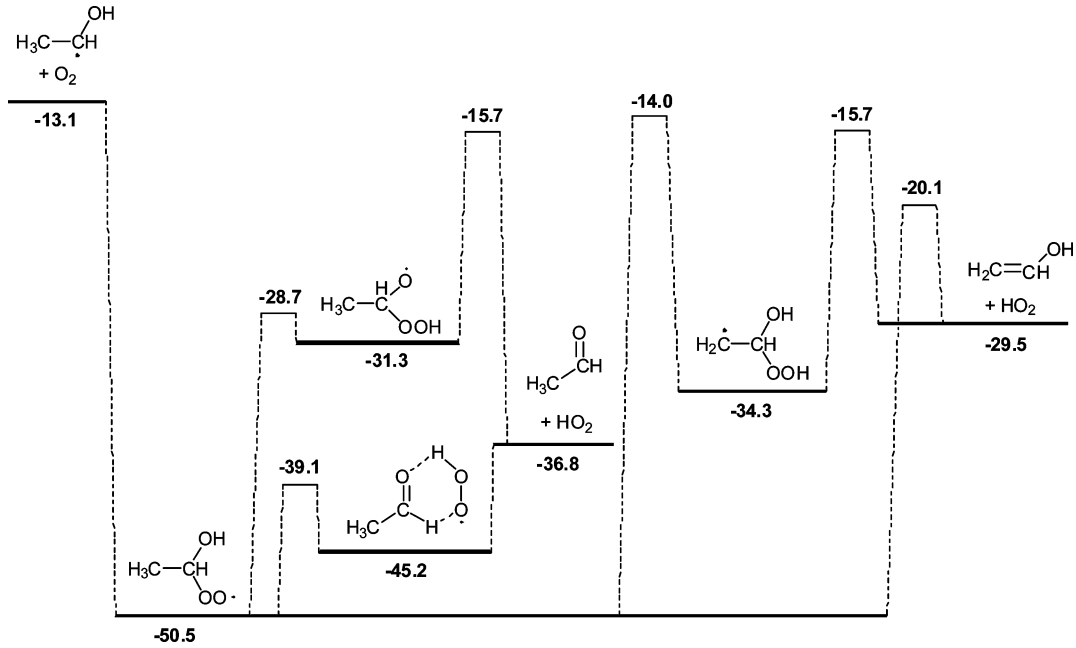

Figure 1. Energy diagram for the α-hydroxyethyl + O_2 reaction mechanism. Enthalpies of formation in kilocalories per mole.

formaldehyde + HO_2.[16,17] Following HO_2 elimination, a weakly bound complex between HO_2 and acetaldehyde forms (termed $CH_3CHO\cdots HOO$). This complex dissociates to its products with a barrier of around 10 kcal mol^{-1}. Alternatively, an intramolecular hydrogen shift from the hydroxy group to the peroxy radical site gives the α-hydroperoxy−ethoxy radical (CH_3-$CH(O^{\bullet})OOH$) with a significantly higher barrier of 21.8 kcal mol^{-1}. This radical dissociates to acetaldehyde + HO_2 with a barrier of 15.6 kcal mol^{-1} (2.6 kcal mol^{-1} below the entrance channel).[29] Pathway II to acetaldehyde + HO_2 is not expected to be of major significance, although collision stabilization of the hydroperoxide intermediate formed by HO_2 addition to the carbonyl may be an important process.

(ii) $CH_2CHOH + HO_2$. Two pathways are available to vinyl alcohol + HO_2 in the α-hydroxyethyl + O_2 reaction mechanism. The α-hydroxy−ethylperoxy radical can undergo an intramolecular hydrogen shift from the methyl carbon to the peroxy group, yielding the 2-hydroxy-2-hydroperoxy−1-ethyl radical ($C^{\bullet}H_2CH(OOH)OH$) with a 36.5 kcal mol^{-1} barrier (only 0.9 kcal mol^{-1} below the entrance channel). This radical can dissociate to vinyl alcohol ($CH_2{=}CHOH$) + HO_2 (18.6 kcal mol^{-1} barrier) or undergo reverse reaction to the α-hydroxy−ethylperoxy radical (20.3 kcal mol^{-1} barrier). Vinyl alcohol is also formed directly from the α-hydroxy−ethylperoxy radical via a concerted, molecular elimination of HO_2. This second pathway provides a lower energy route to vinyl alcohol formation (30.4 kcal mol^{-1} barrier), which lies 7.0 kcal mol^{-1} below the entrance channel energy.

(iii) CH_3 + CH(OH)=O + O. A higher energy pathway available to the α-hydroxy−ethylperoxy radical involves O−O bond dissociation, with a loose, barrierless transition state. These reactions can become important at higher temperatures, as the unfavorable activation energy can be compensated by a large preexponential factor.[28,30] This bond dissociation reaction produces the α-hydroxy−ethoxy radical ($CH_3CH(O^{\bullet})OH$) + O (^3P). Following this dissociation step, the low-energy β scission of the $CH_3CH(O^{\bullet})OH \rightarrow CH_3 + CH(OH){=}O$ reaction should proceed quantitatively from the α-hydroxy−ethoxy radical. This high-energy channel is not depicted in our energy diagram (Figure 1) as it was revealed to be of little significance. In the urban troposphere the α-hydroxy-ethylperoxy radical can also react with NO to form this α-hydroxy-ethoxy radical, providing a potential pathway to tropospheric carboxylic acid formation.

TABLE 1: Standard Enthalpies of Formation for Species in the α-Hydroxyethyl + O_2 Reaction Mechanism

species	$\Delta_f H^\circ_{298}$[a]	species	$\Delta_f H^\circ_{298}$[a]
$CH_3C^{\bullet}HOH$	−13.1	O	59.567[25]
$CH_3CH(OO^{\bullet})OH$	−50.5	HO_2	2.94[33]
$CH_3CH(O^{\bullet})OOH$	−31.3	TS1	−28.7
$C^{\bullet}H_2CH(OOH)OH$	−34.3	TS2	−17.1
$CH_3CH(O^{\bullet})OH$	−50.8	TS3	−39.1
$CH_3CH{=}O\cdots HOO^{\bullet}$	−45.2	TS4	−14.0
$CH_3CH{=}O$	−39.72 [31]	TS5	−15.7
$CH_2{=}CHOH$	−30.0 [32]	TS6	−20.1
O_2	0		

[a] Calculated at the G3B3 level. Units: kcal mol^{-1}.

We briefly discuss some higher energy pathways which were evaluated in our reaction analysis; these are discounted due to prohibitively high reaction barriers. These reaction pathways may be of fundamental interest but do not appear to be of importance to the α-hydroxyethyl + O_2 reaction mechanism. First, the 2-hydroxy-2-hydroperoxy−1-ethyl radical can also dissociate to hydroxy−ethylene oxide (cyclo-$(CH_2OCH)OH$) + OH. The barrier for this reaction is around 37 kcal mol^{-1}, or 16 kcal mol^{-1} above the entrance channel energy. Second, there are two pathways to the vinylperoxy radical ($CH_2{=}CHOO^{\bullet}$), via H_2O elimination in both the α-hydroxy−ethylperoxy and 2-hydroxy-2-hydroperoxy−1-ethyl radicals. These respective pathways occur with barriers of 35 and 15 kcal mol^{-1} above the entrance channel.

Thermochemical Properties. Standard enthalpies of formation ($\Delta_f H^\circ_{298}$) have been calculated for all stable species, radical intermediates, and transition states involved in the reaction of the α-hydroxyethyl radical with O_2, and are listed in Table 1. Enthalpies are calculated at the G3B3 level from atomization work reactions. Literature enthalpies of formation have been used for the species O_2, CH_3CHO,[31] CH_2CHOH,[32] O,[25] and HO_2.[33] The combined G3B3/experimental reaction and activation enthalpies used in this study generally compare well with the

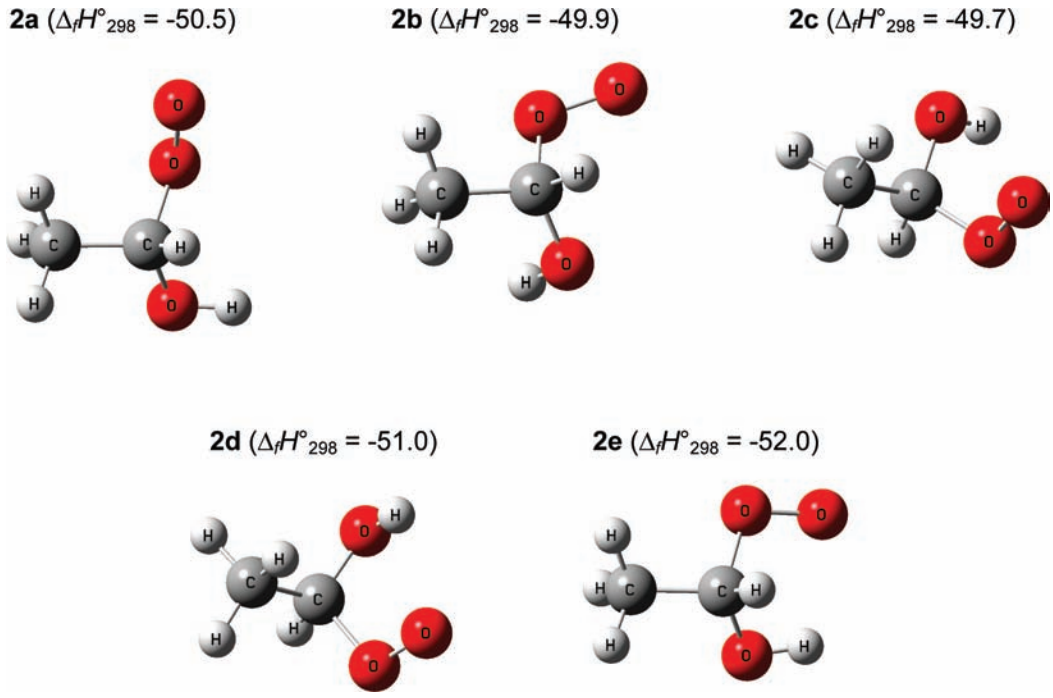

Figure 2. Conformers of the α-hydroxy−ethylperoxy radical. Enthalpies of formation in kilocalories per mole, calculated at the G3B3 level.

QCISD(T) and MRCI values used by Zádor et al.[15] in their study of the α-hydroxyethyl + O_2 reaction (see Supporting Information).

The α-hydroxy−ethylperoxy radical exhibits several conformations, including two which appear to be stabilized by an intramolecular hydrogen bond (IHB) between the hydroxy hydrogen atom and the terminal peroxy oxygen atom (this may more formally be a nonbonded dipole−dipole interaction but is referred to here as an IHB). Each of the identified conformers is illustrated in Figure 2, along with calculated enthalpies of formation. We find that the enthalpies vary little between conformers, with structure **2e** being the most stable ($\Delta_f H°_{298}$ = −52.0), and **2a** the most stable non-hydrogen-bonded structure ($\Delta_f H°_{298}$ = −50.5). In analyzing the kinetics of the α-hydroxyethyl + O_2 reaction, we only consider the lowest energy non-hydrogen-bonded conformation of the α-hydroxy−ethylperoxy radical (i.e., structure **2a** in Figure 2). Structure **2a** is expected to best describe the energy of the activated α-hydroxy−ethylperoxy radical population in our calculations. Preliminary rate constant calculations featuring structure **2e** demonstrate that the presence of the intramolecular hydrogen bond has little effect on the rate constants, with preexponential factors being around 1.2 times larger when reaction proceeds from **2e** rather than **2a**.

Entropy and heat capacity values have been determined for all molecules as a function of temperature, with consideration of internal rotational degrees of freedom. $S°_{298}$ and $C_p(T)$ from 300 to 2000 K are listed for all molecules and transition states in the Supporting Information. Products of the α-hydroxy−ethylperoxy → $CH_3CH(O^•)OH$ + O reaction are not included, as this reaction is modeled using literature rate parameters.

Variational Transition State Theory Analysis. Variational TST analysis has been performed to determine rate constants for the barrierless α-hydroxyethyl + O_2 association reaction and for the reverse dissociation process. A potential energy scan along the dissociating C−OO bond in α-hydroxy−ethylperoxy was calculated at the UB3LYP/6-31G(d) level and then multiplicatively scaled to give accurate relative energies. We identify a very loose transition state, with the transition-state structure approaching the energy of the dissociation products at a C−OO bond length of ca. 5−6 Å.

Rate constants have been calculated for the α-hydroxyethyl + O_2 reaction in the forward and reverse directions, as a function of temperature (300−2000 K) and transition-state structure. Rate constants were calculated at each point along the potential in 0.1 Å intervals, for C−O distances between 2.29 and 4.09 Å. The variational transition state is found to occur at a C−O bond length of 3.99 Å at 300 K, 3.29 Å at 400−900 K, 2.79 Å at 1000−1100 K, and 2.39 Å at 1200−2000 K. Rate constants were also calculated at intervening structures, but they were not found to contribute to the minimum rate constant.

Rate constants as a function of temperature are plotted in Figure 4 for the four contributing transition-state structures. Included in Figure 4 is a solid line denoting the minimum (variational) rate constant and a dashed line indicating an empirical three-parameter Arrhenius fit of $k(T)$. From Figure 4 we notice that the variational rate constant exhibits an inflection at around 700−1400 K. This appears to be an artifact of the VTST analysis, due to the step size (0.1 Å) of the potential energy scan. To obtain an adequate rate expression for $k(T)$, we have fit rate constants for the forward association reaction to the rate parameters E_a, A', and n by neglecting the values between 800 and 1500 K; this is justified when one considers that the variational analysis only ever identifies an upper bound to the actual rate constant. The reverse dissociation reaction, which is dominated by the relatively large reaction enthalpy (activation energy) of 37 kcal mol^{-1}, was well-described by the parameters E_a, A', and n across the entire temperature range. The above analysis provides the rate equation $k/(cm^3\ mol^{-1}\ s^{-1})$ = $4.05 \times 10^{13}(T/K)^{-0.310}\ \exp(169/(T/K))$ for the forward association reaction and $k/s^{-1} = 1.12 \times 10^{25}(T/K)^{-2.97}\ \exp(-19540/(T/K))$ for the reverse dissociation reaction.

Similar analysis was performed for the $CH_3CHO + HO_2 \rightarrow CH_3CHO\cdots HOO$ association reaction and its reverse dissociation. The minimum energy potential for this barrierless reaction, obtained by scanning along the $CH_3CHO-O(H)O$ coordinate, is provided in the Supporting Information. The transition-state

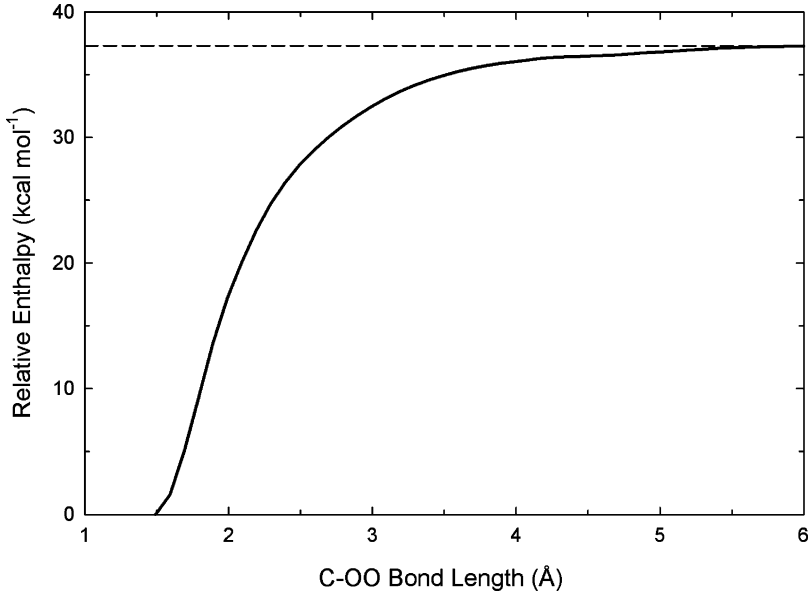

Figure 3. Potential energy surface for dissociation of the C−OO bond in the α-hydroxy−ethylperoxy radical. Calculated at the B3LYP/6-31G(d) level, scaled by the G3B3 298 K reaction enthalpy. Enthalpy levels relative to the α-hydroxy−ethylperoxy radical. Dashed line indicates enthalpy of infinitely dissociated products.

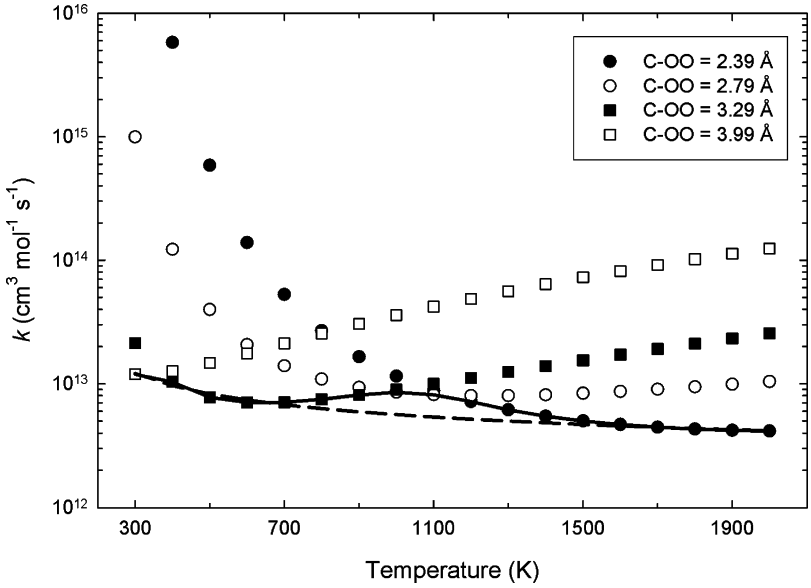

Figure 4. Rate constants as a function of temperature for contributing transition-state structures in the barrierless α-hydroxyethyl + O_2 association reaction. The solid line indicates variational (minimum) rate constant; the dashed line indicates a three-parameter Arrhenius fit of the variational rate constant.

energy approaches that of the infinitely separated products to within around 1 kcal mol^{-1} for an O−O separation distance of 6 Å, and the variational transition state is located between the 4.3 and 3.2 Å structures from 300 to 2000 K. Fitting the variational rate constants to a three-parameter rate law, we obtain $k/s^{-1} = 3.79 \times 10^{20}(T/K)^{-2.04}$ exp(−4280/(*T*/K)) for the dissociation reaction and $k/(cm^3\ mol^{-1}\ s^{-1}) = 3.57 \times 10^{11}(T/K)^{0.429}$ exp(530/(*T*/K)) for the association process.

Transition States and Kinetic Parameters. Transition states have been identified for each elementary reaction in the α-hydroxyethyl + O_2 mechanism proposed in Figure 1, and the structures are depicted in Figure 5. Enthalpies, entropies, and heat capacities for each transition state are provided as Supporting Information. Elementary high-pressure-limit rate parameters (E_a, A', n) have been determined for each reaction between 300 and 2000 K, as provided in Table 2. Parameters for the barrierless reactions are from the above VTST analysis. Rate parameters for the barrierless O−O bond dissociation in α-hydroxyethyl (which turns out to be a relatively unimportant reaction channel) are not calculated here. Instead, the rate constant is estimated as $k^\infty = 2.98 \times 10^{15}T^{-0.090}$ exp(−61.60/*RT*), based upon O−O scission in the ethylperoxy radical.[34] Preliminary QRRK calculations featuring this O−O dissociation reaction demonstrated that it was an unimportant process, and it is not considered any further.

Reaction Kinetics, Products, and Discussion. Using the above-determined thermodynamic and kinetic properties, we have performed RRKM modeling for the reaction kinetics of the chemically activated α-hydroxyethyl + O_2 system in the temperature range of 300−2000 K and for pressures of

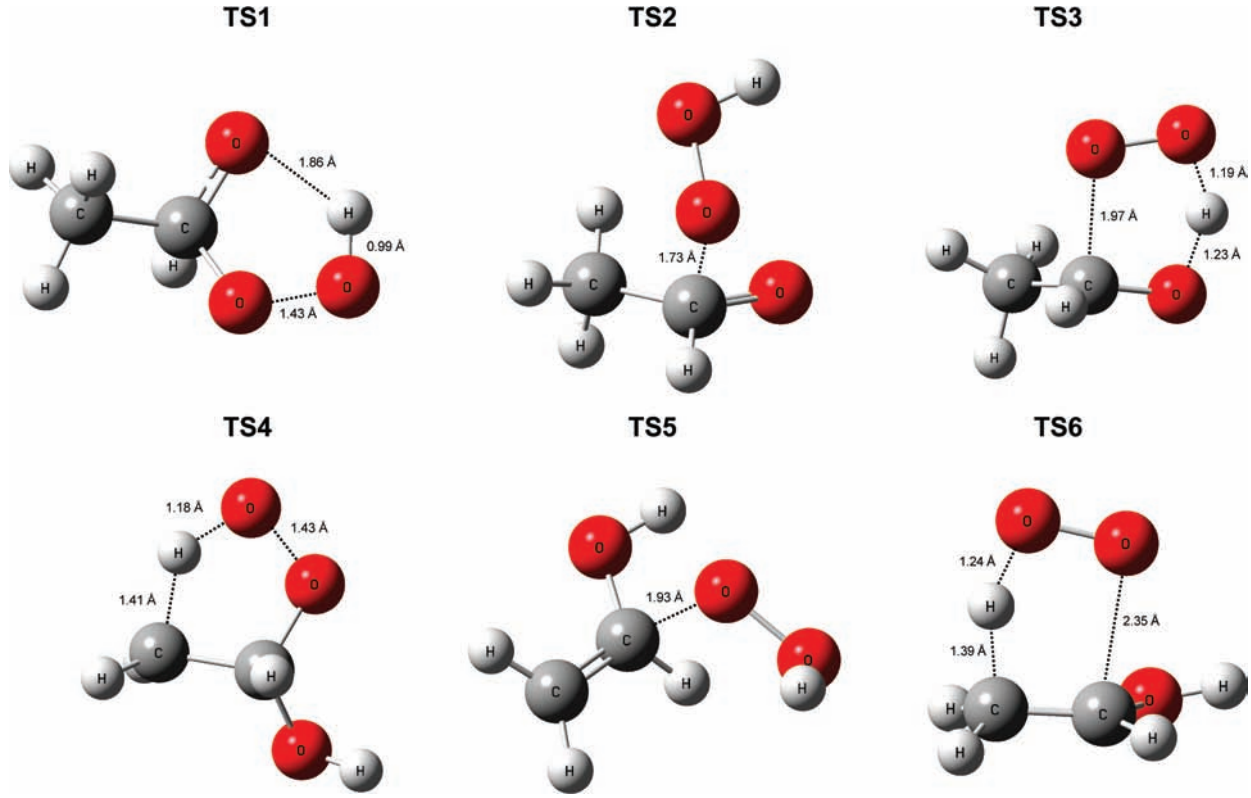

Figure 5. Transition states identified in the α-hydroxyethyl + O_2 reaction mechanism. Transition-state numbering is defined in Table 2.

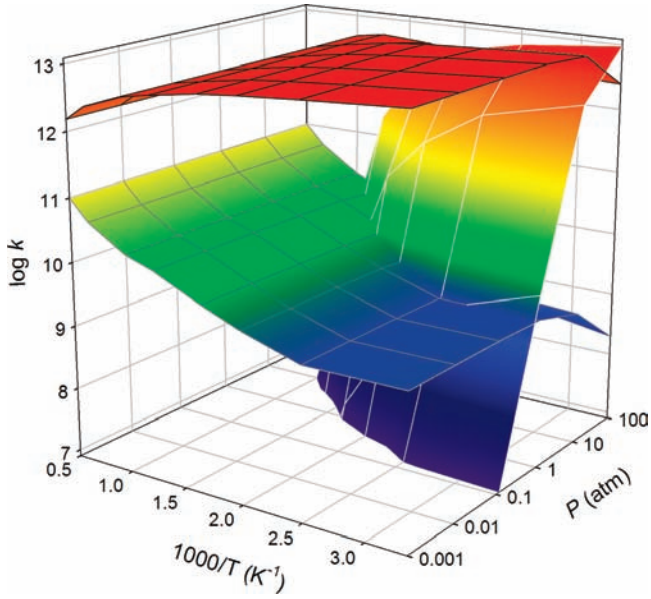

Figure 6. Rate constants (k, $cm^3\ mol^{-1}\ s^{-1}$) as a function of temperature and pressure for formation of acetaldehyde + HO_2 (black lines), vinyl alcohol + HO_2 (gray lines), and stabilized $C_2O_3H_5$ radicals (white lines), in the reaction of α-hydroxyethyl + O_2.

0.001−100 atm. Figure 6 presents calculated rate constants for each important pathway as a function of temperature and pressure. Acetaldehyde and vinyl alcohol formation are presented as the sum of the concerted (I) and stepwise (II) channels, while $C_2H_5O_3$ radical stabilization is the sum of the α-hydroxy−ethylperoxy, α-hydroperoxy−ethoxy, and 2-hydroxy-2-hydroperoxy−1-ethyl radical quenching channels. Branching ratios for the major forward reactions at atmospheric pressure are provided in Figure 7.

We identify the only important new product sets in the α-hydroxyethyl + O_2 reaction as acetaldehyde + HO_2, vinyl alcohol + HO_2, and stabilized $C_2H_5O_3$ radicals. Figure 6 reveals that acetaldehyde formation generally decreases with increasing temperature, while vinyl alcohol formation increases with increasing temperature. However, at 2000 K the rate constant for vinyl alcohol + HO_2 formation is still around an order of magnitude below the acetaldehyde + HO_2 value, for all studied pressures.

At atmospheric temperatures and pressures, stabilization of $C_2H_5O_3$ radicals rivals the vinyl alcohol + HO_2 pathway, but both are relatively unimportant compared to acetaldehyde + HO_2. Stabilization of radical intermediates only becomes the dominant process at around 50 atm (and above) and 500 K (and below), and these radicals will not exist at high concentrations in practical combustion systems. Furthermore, the lifetime of stabilized α-hydroxy−ethylperoxy radicals will be relatively short; the half-life for decomposition to CH_3CHO + HO_2 is calculated as only 0.5 ms at 300 K. The higher energy ethyl−hydroperoxide radical is more stable (half-life of 10 s at 300 K and 3 ms at 400 K) but is present in small quantities at such low temperatures, due to the relatively high reaction barrier for its formation compared to concerted acetaldehyde + HO_2 formation.

Our discovery that $C_2H_5O_3$ radical stabilization is relatively unimportant is a significant result, as it precludes the further oxidation of these radical intermediates, a process involved in cool flame phenomena and engine knock, and a contributor to NTC ignition behavior. One such reaction which is eliminated here is the oxidation of alkylhydroperoxide (QOOH) radicals, known as a major chain branching process in hydrocarbon combustion through the production of two reactive hydroxyl radicals. For ethane,[35] this mechanism takes the following form, or similar:

$$CH_3CH_2^{\bullet} + O_2 \rightarrow CH_3CH_2OO^{\bullet}$$

$$CH_3CH_2OO^{\bullet} \rightarrow C^{\bullet}H_2CH_2OOH \quad \text{(i.e., QOOH)}$$

$$C^{\bullet}H_2CH_2OOH + O_2 \rightarrow {}^{\bullet}OOCH_2CH_2OOH$$

$${}^{\bullet}OOCH_2CH_2OOH \rightarrow \ldots \rightarrow 2HO^{\bullet} + CH_2O + HC^{\bullet}O$$

$$\text{net:} \quad CH_3CH_2^{\bullet} + 2O_2 \rightarrow 2HO^{\bullet} + CH_2O + HC^{\bullet}O$$

Further chain branching pathways which are unimportant here include RO−OH dissociation in the hydroperoxide alkyl radical and hydrogen abstraction followed by OH dissociation in the alkyl peroxy radical. The lack of $C_2H_5O_3$ radical production in the α-hydroxyethyl + O_2 reaction might explain the anomalously long ignition delays measured for ethanol relative to ethane, especially at lower temperatures.[1,36] When ethanol is blended with lower octane hydrocarbon fuels (isooctane, *n*-heptane, etc.), we expect hydrocarbon radicals to abstract the weak α hydrogen atom from ethanol, limiting their chain-branching oxidation via the above $R^{\bullet} + 2O_2$ mechanism (this chain branching process is even more significant in longer chain alkanes such as *n*-heptane, due to reduced ring strain in transition states for intramolecular hydrogen abstraction). This helps explain why ethanol delays the onset of autoignition and the NTC regime when blended with hydrocarbon fuels.[37]

Our finding that $C_2H_5O_3$ radicals are short-lived is also of relevance to the atmospheric chemistry of carbonyl compounds. It has been proposed that α-hydroxyalkyl type radicals will be important aldehyde and ketone sinks in the atmosphere, via their reactions with HO_2.[18] Our results suggest that this process will only become important for acetaldehyde (and, by analogy, for the larger *n*-aldehydes) at very high NO concentrations (tens of ppm). Further kinetic modeling of these systems is, however, required to ascertain the relative importance of these reaction processes.

From Figure 7 we observe that at atmospheric pressure the dominant forward reaction channel at all considered temperatures is the concerted formation of acetaldehyde + HO_2. This pathway is found to constitute close to 100% of the forward reaction flux at low temperatures and around 90% or more at higher temperatures. Acetaldehyde formation is almost entirely due to pathway I, although the stepwise hydroperoxide pathway (II) provides some small contribution at high temperatures. The next most important reaction is for reverse dissociation to α-hydroxyethyl + O_2 (not included in Figure 7), although this process corresponds to no net reaction. On the basis of the above results, the α-hydroxyethyl + $O_2 \rightarrow CH_3CHO + HO_2$ reaction will be an important process in ethanol combustion, and the products of this reaction will significantly impact the combustion kinetics.

Hydroperoxyl radicals (HO_2) are important chain-branching species in combustion systems, due to the reaction sequence

$$HOO^{\bullet} + RH \rightarrow HOOH + R^{\bullet}$$

$$HOOH + M \rightarrow 2HO^{\bullet} + M$$

$$\text{net:} \quad HOO^{\bullet} + RH \rightarrow 2HO^{\bullet} + R^{\bullet}$$

Hydrogen peroxide decomposes to $2HO^{\bullet}$ with a moderate activation energy (ca. 46 kcal mol^{-1}). During combustion, the H_2O_2 lifetime becomes short for temperatures of around 1000−1100 K and above, where it will lead to ignition if present at high enough concentrations. The above process is in competition with chain-terminating bimolecular reactions of HO_2 with H (→$H_2 + O_2$), OH (→$H_2O + O_2$), and HO_2 (→$H_2O_2 + O_2$). H_2O_2 will also participate in bimolecular reactions with, e.g., H and OH radicals.

Acetaldehyde, a secondary oxidation product of ethanol, will also play a role in low-temperature autoignition behavior. As well as being an important reaction intermediate in ethanol combustion, acetaldehyde is a significant toxic atmospheric pollutant. Indeed, it has been suggested that conversion from gasoline to E85 ethanol fueled vehicles would result in increased health risks, principally due to acetaldehyde emissions.[19] It is therefore critical that we understand acetaldehyde formation and destruction mechanisms during ethanol combustion. Acetaldehyde is well-known to demonstrate two-stage ignition and can sustain a cool flame at around 500−600 K. Acetaldehyde combustion is initiated by acetyl radical (CH_3CO) formation; oxidation of this radical to peracetic acid ($CH_3C(=O)OOH$), followed by chain-branching decomposition to $CH_3 + OH + CO_2$ is largely responsible for cool (first-stage) ignition.[38] Hot (second-stage) ignition is due to thermal decomposition of acetaldehyde to $CH_3 + HCO$ (BDE = 84.5 kcal mol^{-1}),[31] as well as the dissociation of H_2O_2.[38] Due to its relatively weak $CH_3C(=O)-H$ and $H-CH_2C=O$ bonds (88.8 and 95.5 kcal mol^{-1}),[31] acetaldehyde will readily undergo abstraction reactions to the acetyl (CH_3CO) and vinoxy (CH_2CHO) radicals. The acetyl radical will predominantly dissociate to $CH_3 + CO$, while the vinoxy radical will undergo unimolecular reactions to $CH_3 + CO$ and to ketene ($CH_2=C=O$) + H. Both species will also participate in oxidation and radical addition reactions.

Following acetaldehyde, the next most important reaction channel in the chemically activated α-hydroxyethyl + O_2 system is vinyl alcohol formation (+HO_2), principally via the concerted mechanism. Both the concerted and stepwise pathways increase in importance with increasing temperature, and our calculations predict that 6% of the α-hydroxyethyl + O_2 reaction will produce vinyl alcohol + HO_2 at 2000 K, dropping to only 0.3% at 800 K. Vinyl alcohol is an important combustion intermediate

TABLE 2: High-Pressure-Limit Elementary Rate Parameters for Reactions in the α-Hydroxyethyl + O_2 System[a]

	$E_{a,f}$	A'_f	n_f	$E_{a,r}$	A'_r	n_r
$CH_3C^{\bullet}HOH + O_2 \rightleftharpoons CH_3CH(OO^{\bullet})OH$	−0.336	4.05×10^{13}	−0.310	38.83	1.12×10^{25}	−2.974
$CH_3CH(OO^{\bullet})OH \rightleftharpoons CH_3CH(O^{\bullet})OOH$ [TS1]	21.64	8.62×10^{8}	0.822	2.94	4.38×10^{10}	0.414
$CH_3CH(O^{\bullet})OOH \rightarrow CH_3CHO + HO_2$ [TS2]	15.86	7.56×10^{15}	−0.483	19.95	3.45×10^{4}	2.253
$CH_3CH(OO^{\bullet})OH \rightleftharpoons CH_3CH{=}O\cdots HOO^{\bullet}$ [TS3]	10.63	2.60×10^{8}	1.128	5.63	4.65×10^{7}	1.036
$CH_3CH{=}O\cdots HOO^{\bullet} \rightarrow CH_3CHO + HO_2$	8.50	3.79×10^{20}	−2.04	−1.05	3.57×10^{11}	0.429
$CH_3CH(OO^{\bullet})OH \rightleftharpoons C^{\bullet}H_2CH(OOH)OH$ [TS4]	34.24	6.65×10^{5}	1.890	17.37	4.85×10^{6}	1.325
$C^{\bullet}H_2CH(OOH)(OH) \rightarrow CH_2CHOH + HO_2$ [TS5]	18.97	3.42×10^{11}	0.454	11.15	2.27×10^{2}	2.949
$CH_3CH(OO^{\bullet})OH \rightarrow CH_2CHOH + HO_2$ [TS6]	30.05	2.82×10^{8}	1.361	5.36	$1.37 \times 10^{\circ}$	3.291
$CH_3CH(OO^{\bullet})OH \rightarrow CH_3CH(O^{\bullet})OH + O$	61.60	2.98×10^{15}	−0.090			

[a] $k^{\infty} = A'T^{n} \exp(-E_a/RT)$; units: unimolecular reactions: s^{-1}, bimolecular reactions: $cm^3\ mol^{-1}\ s^{-1}$, energy: kcal mol^{-1}, T(K).

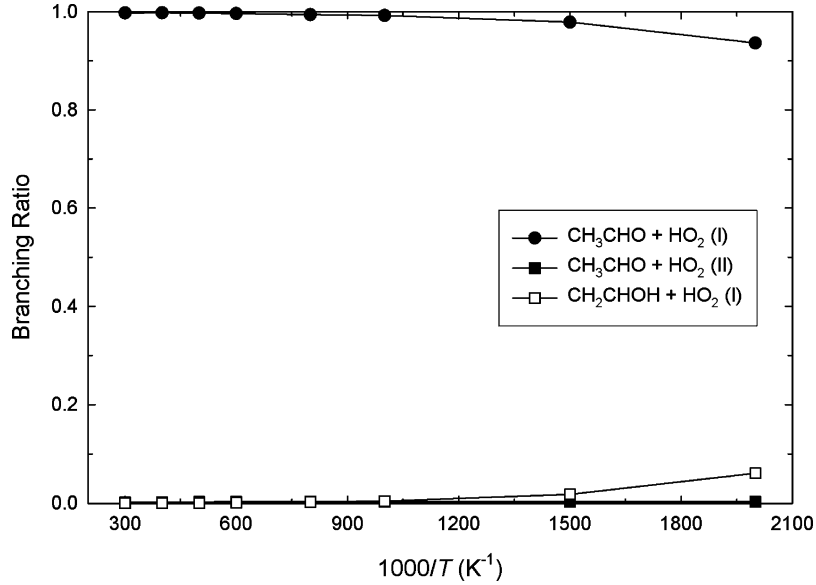

Figure 7. Branching ratios for important reaction channels in the α-hydroxyethyl + O_2 reaction. $P = 1$ atm.

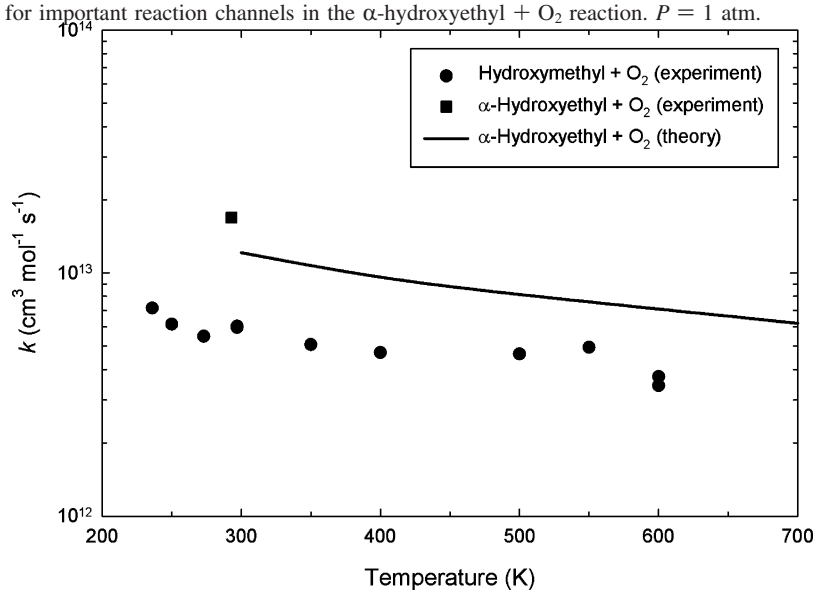

Figure 8. Comparison of the α-hydroxyethyl + $O_2 \rightarrow CH_3CHO + HO_2$ and the hydroxymethyl + $O_2 \rightarrow CH_2O + HO_2$ rate constants at low temperatures. Calculated (theory) values from this study. Experimental values from Schocker et al.[16] (hydroxymethyl) and Miyoshi et al.[40] (hydroxyethyl).

which has until recently been neglected from combustion mechanisms.[39] Interestingly, vinyl alcohol formation is found to be enhanced by the addition of ethanol to propene flames,[20] and the present mechanism provides a pathway to increased enol formation in alcohol flames. Vinyl alcohol will undergo a keto−enol tautomerization to acetaldehyde, with $k/s^{-1} = 1.05 \times 10^9 (T/K)^{1.202} \exp(-33400/(T/K))$,[32] but due to the large activation energy (66 kcal mol^{-1}) this mechanism will only become important at high temperatures.

Comparison with Experiment. We compare the results of this study to previous experimental findings. Miyoshi et al.[40] measured a rate constant of 1.7×10^{13} cm^3 mol^{-1} s^{-1} for the α-hydroxyethyl + O_2 reaction at 293 K. While to our understanding no experimental data are available for this reaction at higher temperatures, there does exist a good deal of data for the analogous hydroxymethyl + $O_2 \rightarrow CH_2O + HO_2$ reaction. While both reactions are not expected to proceed at exactly the same rate, due to differences in chemistry of the two systems (hydroxyethyl is reacting at a secondary carbon radical site, versus a primary site in the hydroxymethyl), they should exhibit similar trends. Figure 8 shows a comparison between the calculated α-hydroxyethyl + $O_2 \rightarrow CH_3CHO + HO_2$ reaction rate (at 1 atm), the 293 K measurement of Miyoshi et al.,[40] and the experimental values for the similar hydroxymethyl + $O_2 \rightarrow CH_2O + HO_2$ reaction as measured by Schocker et al.[16] There exist numerous studies of the hydroxymethyl + O_2 reaction rate (see ref 16), which are all in generally good agreement, and for clarity only the most recent experimental results are used here. From Figure 8 we find that the calculated and experimental rate constants for the two respective reactions are in relative agreement, with the α-hydroxyethyl rate constants (both experimental and theoretical) being larger than the hydroxymethyl values by around a factor of 5. This difference is within the combined error of the calculations and the experiments, and we are therefore unable to distinguish any significant difference between the hydroxyethyl and the hydroxymethyl systems, with respect to aldehyde formation. Of note, the small negative temperature dependence observed for the experimental results is accurately reproduced by the present calculations.

TABLE 3: Input Rate Parameters for Important Reactions in the α-Hydroxyethyl + O_2 System ($P = 1$ atm)[a]

	E_a (kcal mol^{-1})	A'	n
$CH_3C^{\bullet}HOH + O_2 \rightarrow CH_3CHO + HO_2$	0.839	5.28×10^{17}	−1.638
$CH_3C^{\bullet}HOH + O_2 \rightarrow CH_2CHOH + HO_2$	−0.296	7.62×10^{2}	2.446
$CH_3C^{\bullet}HOH + O_2 \rightarrow CH_3CH(OO^{\bullet})OH$	21.19	5.63×10^{109}	−34.200
$CH_3C^{\bullet}HOH + O_2 \rightarrow CH_3CH(O^{\bullet})OOH$	12.08	5.42×10^{60}	−19.626
$CH_3C^{\bullet}HOH + O_2 \rightarrow C^{\bullet}H_2CH(OOH)OH$	4.46	2.02×10^{48}	−15.434

[a] k (cm^3 mol^{-1} s^{-1}) $= A'T^n \exp(-E_a/RT)$.

Rate constants calculated here compare well with the theoretical values of Zádor et al.[15] While rate expressions were not provided in their study, at 400 K the rate constant is around 1.2×10^{13} cm^3 mol^{-1} s^{-1}, whereas we obtain a value of 9.6×10^{12} cm^3 mol^{-1} s^{-1} at 400 K and 1 atm. The α-hydroxyethyl + O_2 reaction proceeds at a rate somewhat greater than the hydroxymethyl + O_2 reaction (agreeing with the room-temperature experimental result of ref 40), with a similar negative activation energy.[41] Our results deviate significantly from the rate expression used in the kinetic model of Marinov at moderate to high temperatures, as do the results of Zádor et al. This provides further support for the use of an updated rate expression for the α-hydroxyethyl + $O_2 \rightarrow$ acetaldehyde + HO_2 reaction in modeling ethanol oxidation.

Input Rate Parameters. Pressure-dependent input rate parameters (A', n, E_a) for the construction of kinetic models have been determined for important reaction pathways in the α-hydroxyethyl + O_2 mechanism, for $P = 0.001-100$ atm. The results at 1 atm are listed in Table 3, with the remaining values in the Supporting Information. Rate constants are provided for reaction to acetaldehyde + HO_2 and vinyl alcohol + HO_2, as well as for formation of the three stabilized intermediates (the short-lived $CH_3CHO\cdots HOO$ complex is not included). Only low-temperature (<800 K) rate constants were used to fit the rate parameters for intermediate stabilization, above which point they were negligible. Fitted rate constants for the acetaldehyde + HO_2 reaction reproduce the original calculated values to within a factor of 0.8−1.3. Errors are slightly larger for the vinyl alcohol + HO_2 reaction, with rate constant fits differing by a factor of 0.7−1.7. Accurately fitting rate expressions for the formation of collision-stabilized $C_2O_3H_5$ adducts proved more difficult, and here the fitted rate expressions reproduce the calculated rate constants to within an order of magnitude. It should be noted that values of the activation energies (E_a) and preexponential factors ($A'T^n$) reported in Table 3 have little physical meaning in the context of the Arrhenius equation and are simply used as a technique to reproduce the calculated rate constants at different temperatures and pressures.

Conclusions

The α-hydroxyethyl + O_2 reaction is shown to be important in the autoignition and oxidation of ethanol and in the atmospheric chemistry of aldehydes, ketones, and enols. Our main findings are summarized as follows:

(i) The chemically activated α-hydroxyethyl + O_2 reaction proceeds almost exclusively to acetaldehyde + HO_2, due to a very low energy molecular elimination pathway, resulting in essentially no collision stabilization of $C_2H_5O_3$ radicals. This precludes several chain branching processes which are important in alkane ignition, including the $R^{\bullet} + 2O_2$ mechanism which is known to be controlling in the two-stage autoignition of ethane. Our findings therefore explain why ignition delays for ethanol are longer than those for ethane (especially at lower temperatures), despite ethanol having the weaker C−C bond. Chain branching reactions involving acetaldehyde and H_2O_2 are suggested to be significant at lower temperatures, where the high-energy C−C bond scission is unimportant.

(ii) Vinyl alcohol + HO_2 is a minor, but important, product set in the α-hydroxyethyl + O_2 mechanism. Vinyl alcohol is a recently identified combustion intermediate which is not adequately included in current models of combustion and atmospheric chemistry. It has been recently found that the oxidation of vinyl alcohol contributes to the production of formic acid (a component of acid rain) in the troposphere.

(iii) We propose that the α-hydroxy−ethylperoxy radical will not be an important sink for atmospheric acetaldehyde, as has been previously suggested, due to the low barrier for dissociation to acetaldehyde + HO_2. Further modeling work is required to identify the importance of this reaction process for aldehydes and ketones.

Acknowledgment. J.W.B. and G.d.S. gratefully acknowledge funding from the ExxonMobil Educational Fund and the NJIT Ada C. Fritts Chair. This work was presented in part at the 2007 Meeting of the U.S. Combustion Institute and at the 2007 Eastern States Meeting of the U.S. Combustion Institute.

Supporting Information Available: Geometries, frequencies, and G3B3 enthalpies for all stationary points, entropy (S°_{298}) and heat capacity (C_p, 300−2000 K) values, comparison of reaction and activation enthalpies with those of ref 15, minimum energy potential for $CH_3CHO\cdots HOO$ dissociation, and apparent rate parameters for the α-hydroxyethyl + O_2 reaction from 0.001 to 100 atm. This material is available free of charge via the Internet at http://pubs.acs.org.

References and Notes

(1) Cooke, D. F.; Dodson, M. G.; Williams, A. *Combust. Flame* **1971**, *16*, 233.

(2) BDE calculations use the following 298 K heats of formation (kcal mol^{-1}): 52.103 (H);[3] −4.08 (CH_2OH);[4] 35.05 (CH_3);[5] 8.91 (OH);[6] −48.07 (CH_3OH);[7] −56.23 (CH_3CH_2OH);[7] −20.04 (CH_3CH_3).[8]

(3) Chase, M. W., Jr. *J. Phys. Chem. Ref. Data, Monogr.* **1998**, *9*, 1.

(4) Ruscic, B.; Berkowitz, J. *J. Phys. Chem.* **1993**, *97*, 11451.

(5) Ruscic, B.; Litorja, M.; Asher, R. L. *J. Phys. Chem. A* **1999**, *103*, 8625.

(6) Ruscic, B.; Wagner, A. F.; Harding, L. B.; Asher, R. L.; Feller, D.; Dixon, D. A.; Peterson, K. A.; Song, Y.; Qian, X.; Ng, C.-Y.; Liu, J.; Chen, W.; Schwenke, D. W. *J. Phys. Chem. A* **2002**, *106*, 2727.

(7) Green, J. H. S. *Chem. Ind.* **1960**, 1215.

(8) Pittam, D. A.; Pilcher, G. *J. Chem. Soc., Faraday Trans. 1* **1972**, *68*, 2224.

(9) Dunphy, M. P.; Patterson, P. M.; Simmie, J. M. *J. Chem. Soc., Faraday Trans.* **1991**, *87*, 2549.

(10) Dunphy, M. P.; Simmie, J. M. *J. Chem. Soc., Faraday Trans.* **1991**, *87*, 1691.

(11) Marinov, N. M. *Int. J. Chem. Kinet.* **1999**, *31*, 183.

(12) Li, J.; Kazakov, A.; Dryer, F. L. *Int. J. Chem. Kinet.* **2001**, *33*, 859.

(13) Li, J.; Kazakov, A.; Dryer, F. L. *J. Phys. Chem. A* **2004**, *108*, 7671.

(14) da Silva, G.; Bozzelli, J. W.; Liang, L.; Farrell, J. T. *Proceedings of the 5th U.S. Combustion Meeting*, San Diego, March 2007.

(15) Zádor, J.; Fernandes, R. X.; Georgievskii, Y.; Meloni, G.; Taatjes, C. A.; Miller, J. A. *Proc. Combust. Inst.* **2009**, *32*, 271.

(16) See: Schocker, A.; Uetake, M.; Kanno, N.; Koshi, M.; Tonokura, K. *J. Phys. Chem. A* **2007**, *111*, 6622, and references therein.

(17) (a) Dibble, T. S. *Chem. Phys. Lett.* **2002**, *355*, 193. (b) Olivella, S.; Bofill, J. M.; Solé, A. *Chem.−Eur. J.* **2001**, *7*, 3377. (c) Ramírez-Ramírez, V. M.; Serrano-Andrés, L. S.; Nebot-Gil, I. *Theor. Chem. Acc.* **2006**, *116*, 637.

(18) (a) Hermans, I.; Nguyen, T. L.; Jacobs, P. A.; Peeters, J. *J. Am. Chem. Soc.* **2004**, *126*, 9908. (b) Hermans, I.; Müller, J.-F.; Nguyen, T. L.; Jacobs, P. A.; Peeters, J. *J. Phys. Chem. A* **2005**, *109*, 4303.

(19) Jacobson, M. Z. *Environ. Sci. Technol.* **2007**, *41*, 4150.

(20) Kohse-Höinghaus, K.; Osswald, P.; Struckmeier, U.; Kasper, T.; Hansen, N.; Taatjes, C. A.; Wang, J.; Cool, T. A.; Gon, S.; Westmoreland, P. R. *Proc. Combust. Inst.* **2007**, *31*, 1119.

(21) Archibald, A. T.; McGillen, M. R.; Taatjes, C. A.; Percival, C. J.; Shallcross, D. E. *Geophys. Res. Lett.* **2007**, *34*, L21801.

(22) Keene, W. C.; Galloway, J. N. *Atmos. Environ.* **1984**, *18*, 2491.

(23) Frisch, M. J.; Trucks, G. W.; Schlegel, H. B.; Scuseria, G. E.; Robb, M. A.; Cheeseman, J. R.; Montgomery, J. A., Jr.; Vreven, T.; Kudin, K. N.; Burant, J. C.; Millam, J. M.; Iyengar, S. S.; Tomasi, J.; Barone, V.; Mennucci, B.; Cossi, M.; Scalmani, G.; Rega, N.; Petersson, G. A.; Nakatsuji, H.; Hada, M.; Ehara, M.; Toyota, K.; Fukuda, R.; Hasegawa, J.; Ishida, M.; Nakajima, T.; Honda, Y.; Kitao, O.; Nakai, H.; Klene, M.; Li, X.; Knox, J. E.; Hratchian, H. P.; Cross, J. B.; Adamo, C.; Jaramillo, J.; Gomperts, R.; Stratmann, R. E.; Yazyev, O.; Austin, A. J.; Cammi, R.; Pomelli, C.; Ochterski, J. W.; Ayala, P. Y.; Morokuma, K.; Voth, G. A.; Salvador, P.; Dannenberg, J. J.; Zakrzewski, V. G.; Dapprich, S.; Daniels, A. D.; Strain, M. C.; Farkas, O.; Malick, D. K.; Rabuck, A. D.; Raghavachari, K.; Foresman, J. B.; Ortiz, J. V.; Cui, Q.; Baboul, A. G.; Clifford, S.; Cioslowski, J.; Stefanov, B. B.; Liu, G.; Liashenko, A.; Piskorz, P.; Komaromi, I.; Martin, R. L.; Fox, D. J.; Keith, T.; Al-Laham, M. A.; Peng, C. Y.; Nanayakkara, A.; Challacombe, M.; Gill, P. M. W.; Johnson, B.; Chen, W.; Wong, M. W.; Gonzalez, C.; Pople, J. A. *Gaussian 03*, Revision D.01, Gaussian: Wallingford, CT, 2004.

(24) Baboul, A. G.; Curtiss, L. A.; Redfern, P. C.; Raghavachari, K. *J. Chem. Phys.* **1999**, *110*, 7650.

(25) Ruscic, B.; Pinzon, R. E.; Morton, M. L.; von Laszevski, G.; Bittner, S. J.; Nijsure, S. G.; Amin, K. A.; Minkoff, M.; Wagner, A. F. *J. Phys. Chem. A* **2004**, *108*, 9979.

(26) Mokrushin, V.; Bedanov, V.; Tsang, W.; Zachariah, M.; Knyazev, V. *ChemRate*, Version 1.5.2; National Institute of Standards and Testing: Gaithersburg, MD, 2006.

(27) Eckart, C. *Phys. Rev.* **1930**, *35*, 1303.

(28) da Silva, G.; Bozzelli, J. W. *J. Phys. Chem. A* **2008**, *112*, 3566.

(29) This transition state follows a more conventional H atom transfer reaction and subsequent β scission and is described in ref 15.

(30) da Silva, G.; Chen, C.-C.; Bozzelli, J. W. *J. Phys. Chem. A* **2007**, *111*, 8663.

(31) da Silva, G.; Bozzelli, J. W. *J. Phys. Chem. A* **2006**, *110*, 13058.

(32) da Silva, G.; Kim, C.-H.; Bozzelli, J. W. *J. Phys. Chem. A* **2006**, *110*, 7925.

(33) Ruscic, B.; Pinzon, R. E.; Morton, M. L.; Srinivasan, N. K.; Su, M.-C.; Sutherland, J. W.; Michael, J. V. *J. Phys. Chem. A* **2006**, *110*, 6592.

(34) Sheng, C. Y.; Bozzelli, J. W.; Dean, A. M.; Chang, A. Y. *J. Phys. Chem. A* **2002**, *106*, 7276.

(35) Bozzelli, J. W.; Sheng, C. *J. Phys. Chem. A* **2002**, *106*, 1113.

(36) Warnatz, J. *Proc. Combust. Inst.* **1992**, *24*, 553.

(37) (a) Xingcai, L.; Yuchun, H.; Linlin, Z.; Zhen, H. *Fuel* **2006**, *85*, 2622. (b) Hou, Y. C.; Lu, X. C.; Zu, L. L.; Ji, L. B.; Huang, Z. *Energy Fuels* **2006**, *20*, 1425. (c) Caton, P. A.; Hamilton, L. J.; Cowart, J. S. *SI Combust. (SAE Special Publ. SP-2127)* **2007**, 15.

(38) (a) Halstead, M. P.; Prothero, A.; Quinn, C. P. *Proc. R. Soc. London, Ser. A* **1971**, *322*, 377. (b) Cavanagh, J.; Cox, R. A.; Olson, G. *Combust. Flame* **1990**, *82*, 15.

(39) Taatjes, C. A.; Hansen, N.; McIlroy, A.; Miller, J. A.; Senosiain, J. P.; Klippenstein, S. J.; Qi, F.; Sheng, L.; Zhang, Y.; Cool, T. A.; Wang, J.; Westmoreland, P. R.; Law, M. E.; Kasper, T.; Kohse-Höinghaus, K. *Science* **2005**, *308*, 1887.

(40) Miyoshi, A.; Matsui, H.; Washida, N. *Chem. Phys. Lett.* **1989**, *160*, 291.

(41) A preliminary report of this work[14] used an incorrect rate constant for the α-hydroxyethyl + O_2 association reaction. This resulted in rate constants for the formation of $CH_3CHO + HO_2$ significantly lower than those reported here and in ref 15.

JP903210A